

Design of Experiment for Measurement of Langevin Function

P. Tuček^{1*}, M. Tučková^{1,2}, E. Fišerová², J. Tuček³, L. Kubáček²

¹Department of Geoinformatics, Faculty of Science, Palacký University in Olomouc

²Department of Mathematical Analysis and Applied Mathematics, Faculty of Science, Palacký University in Olomouc

³Regional Centre of Advanced Technologies and Materials, Department of Experimental Physics, Faculty of Science, Palacký University in Olomouc

The presented study focuses on a confrontation of the theory of regression models and theory of experiment with the real situation of determining properties of magnetic (nano)materials. Their magnetic properties can be deduced by measuring their magnetization, being the fundamental magnetic quantity of an arbitrary (nano)material. The results of the magnetization measurements determine the unknown parameters of a known nonlinear function that characterizes the (nano)material under investigation. Knowledge of the values of the unknown parameters enables to decide whether the (nano)material is suitable or not for a particular application. Thus, in this work, we present a possible approach how to estimate the unknown parameters of the nonlinear function by the regression models, taking into account a relevant linearization criterion. Then, we suggest an appropriate design for the measurement to get better estimators of the parameters.

Keywords: Approximation, nonlinear regression models, linearization, BLUE, D-optimal design of experiment, nanomaterial, hysteresis loop, Langevin function

1. INTRODUCTION

DU TO their high application potential, magnetic materials raise a significant attention of the scientific community [5]. It turns out that if the size of the magnetic material is reduced, below its characteristic size, new physico-chemical properties emerge that are totally different from those exhibited by the material's bulk counterpart [5, 12]. This is caused by a fact that in the nanoworld, the magnetic behaviour of materials is governed by other physical laws than at the macroscopic scale [2]. In almost all cases, we observe a magnetic behaviour that is very promising and attractive for its subsequent practical application.

From the application viewpoint, iron- and iron-oxide-based compounds constitute one of the most important types of magnetic materials [8, 14, 15, 18]. If these compounds are synthesized as nanoparticles they can be utilized in a broad variety of practical branches of human activity (e.g., contrast agents in nuclear magnetic resonance imaging, carriers of drugs, heat mediators in magnetically-induced hyperthermia, tools in cell labelling, magnetic pigments in information storage industry, etc.).

In general, we distinguish two approaches how to synthesize magnetic nanoparticles, i.e., top-down (physical) and bottom-up (chemical) approach [12]. As a result of both synthetic ways, we can prepare various systems of magnetic nanoparticles differing in their sizes, size distributions and shapes and may affect their degree of agglomeration.

Once such a system of nanoparticles is synthesized, it is necessary to study its magnetic properties on which basis we can decide whether the as-synthesized nanoparticle system meets requirements imposed by a given application. From this viewpoint, we look for magnetization (denoted as M) of the

system which represents the basic physical quantity of every magnetic material and/or nanomaterial. The magnetization can be measured in two ways. We recognize temperature-dependent magnetization when the external magnetic field is kept constant and the magnetization is measured within a given temperature range, or field-dependent magnetization when the temperature is kept constant and the magnetization is acquired within a given interval of the magnetic induction (denoted as B) of an external magnetic field. The result of the second approach is the so-called hysteresis loop, being one of the main magnetic characteristics of a magnetic material used for its classification into a group of soft or hard magnetic materials [10]. From the measured hysteresis loop, it is possible to determine several parameters that unambiguously characterize the studied material. On the basis of the values of these parameters, one can decide if the material is suitable or not for the intended application.

Nanosized magnetic materials exhibit one remarkable phenomenon that is known as superparamagnetism and is characterized by a zero value of the coercivity and remanent magnetization [2]. When the magnetic nanomaterial is in the superparamagnetic state, the corresponding hysteresis loop crosses the origin of the M vs. B plot and the upper and lower branch of the hysteresis loop are identical, see Fig. 1.

In most cases, the profile of the superparamagnetic hysteresis loop is described by the well-known Langevin function (for another example of application see [13]) which is given by [2]

$$y_i = \beta_1 \cdot \coth(\beta_2 \cdot x_i) - \frac{\beta_1}{\beta_2 \cdot x_i}, \quad i = 1, \dots, n, \quad (1)$$

where β_1 and β_2 are parameters which represent physical constants unambiguously characterizing the investigated nanomaterial. From the physical viewpoint, the coefficient β_1

*Corresponding author: pavel.tucek@upol.cz

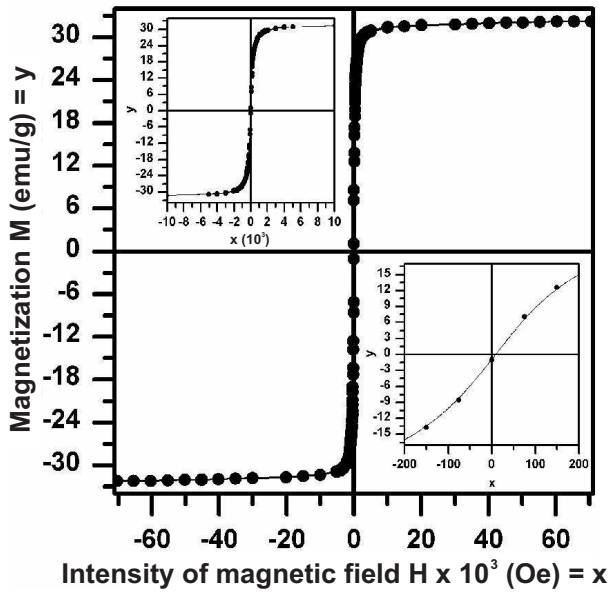


Fig. 1: Example of the hysteresis loop of a nanomaterial in the superparamagnetic state.

stands for the saturation magnetization of a given nanomaterial and is a measure of strength of the nanomaterial magnetic response in external magnetic fields. The coefficient β_2 represents a magnetic moment of a magnetically-active ion in a nanomaterial (i.e., magnetic element that drives the magnetic response of the nanomaterial), divided by the Boltzmann constant and the temperature at which the measurement of the hysteresis loop is performed. The coefficient β_2 reflects the tendency to reach the magnetic saturation; if the value of β_2 is high, small applied magnetic fields are needed to magnetically saturate the given nanomaterial. Thus, in many applications, nanomaterials exhibiting high values of both parameters are highly required.

The aim is thus to find out the estimates of the parameters of this function for data acquired from the physical experiment. Thus, we use a regression model when the nonlinear function is firstly transformed into its linear approximation by the Taylor series expansion. Concurrently, we find the locally D-optimal design of measurement to maximize the accuracy of the found estimators of the unknown parameters and to maximize the economic efficiency of the experiment [16].

In the numerical part, we apply the proposed algorithms to analyze experimental data acquired from the magnetization measurement of spherically-shaped nanoparticles of $\gamma\text{-Fe}_2\text{O}_3$ which were synthesized by a solid-state isothermal decomposition of iron(III) acetate dihydrate (bought from Sigma Aldrich company) in air at 380°C (for synthesis details, see [4]). Prior to the synthesis itself, the iron(III) acetate was homogenized by grinding in an agate mortar resulting in the size distribution of the precursor particles of 1–5 μm . The weight of the precursor powder was 1 g and the reaction time was 1 hour. The size distribution of the as-prepared $\gamma\text{-Fe}_2\text{O}_3$

nanoparticles was found to fall in the range from 5 to 10 nm.

2. EXPERIMENT AND METHODS

A superconducting quantum interference device (SQUID, MPMS XL-7 type, Quantum Design) was used for the magnetization measurements. Hysteresis loop was recorded at 300 K in 150 points of an external magnetic field ranging from -70000 to $+70000$ Oe. Firstly, at each measuring point, three mutually-independent measurements were carried out resulting in 450 values in total. To measure the hysteresis loop, we adopted the following typical measuring procedure. After placing the sample into the magnetometer sample chamber and centering it to get the proper signal, the temperature was set to a value at which the measurement of hysteresis loop was performed (300 K in our case). The magnetometer waited approximately 30 minutes to become stable. Then, each measurement was initiated when a given value of the induction of the external magnetic field was reached; this took 2–5 minutes including multiple measurements at each measuring point. In our case, this measuring process was repeated 150 times.

2.1. Description of a model

From the mathematical viewpoint, we have the values of sample mean magnetization $\bar{\mathbf{y}} = (\bar{y}_1, \bar{y}_2, \dots, \bar{y}_n)'$, measured in the points of the external magnetic field intensity $(x_1, x_2, \dots, x_n)'$. The symbol prime stands for the transposition. In our case, $n = 150$ and \bar{y}_i is an average of three mutually-independent measurements in each x_i . The statistical model is in the form of

$$\bar{\mathbf{y}} = \phi(\beta_1, \beta_2) + \varepsilon, \quad (2)$$

where the i th component of n -dimensional vector ϕ represents the nonlinear Langevin function (1) at the point x_i , $\beta = (\beta_1, \beta_2)'$ denotes the unknown vector parameter and ε is the n -dimensional vector of random errors. The observation vector $\bar{\mathbf{y}}$ is normally distributed with the covariance matrix $\sigma^2 \Lambda^{-1}$. Here Λ stands for the diagonal matrix of $n \times n$ order with the value $\lambda_i r(i)$ on the main diagonal, where $\lambda_i = 1$ and $r(i) = 3$, the former being the weight and the latter being the number of replications of measurements performed at point x_i (measurement has the same weight at any point x_i , each \bar{y}_i is an average of 3 measurements). The parameter $\sigma = 0.002 \text{ Am}^2\text{kg}^{-1}$ and characterizes the accuracy of measurement (the value was adopted from the documentation protocol of the measurement device).

2.2. Linearization of the model

The statistical model (2) is nonlinear. Let us consider approximation β^0 of the parameter β ; The initial value of β^0 was set with respect to the values of parameters β_1 and β_2 derived for various $\gamma\text{-Fe}_2\text{O}_3$ nanoparticle systems and reported in literature. We compared the quadratic approximation with the analytically exact course of the Langevin function. It showed that the quadratic course approximates the real course

of the Langevin function in a sufficiently large neighborhood of a given point β^0 . Since we can choose a sufficiently large neighbourhood \mathcal{O} of the point β^0 such that the true value of β lies in \mathcal{O} and the third derivatives of the Langevin function can be neglected for an arbitrary point $\beta \in \mathcal{O}$, the parametric space of the parameter β can be restricted to the set \mathcal{O} , where the model can be approximated in terms of the quadratic model. In particular,

$$\bar{y} - \phi(\beta_1^0, \beta_2^0) = \mathbf{F}\delta\beta + \frac{1}{2}\kappa(\delta\beta) + \varepsilon, \quad (3)$$

where

$$\begin{aligned} \delta\beta &= \beta - \beta^0 \\ \mathbf{F} &= \frac{\partial\phi(\beta_1^0, \beta_2^0)}{\partial\beta'} \\ \kappa(\delta\beta) &= (\kappa_1(\delta\beta), \dots, \kappa_n(\delta\beta))' \\ \kappa_i(\delta\beta) &= \delta\beta' \mathbf{H}_i \delta\beta \\ \mathbf{H}_i &= \frac{\partial^2\phi(x_i, \beta_1^0, \beta_2^0)}{\partial\beta\partial\beta'}, \quad i = 1, \dots, n. \end{aligned}$$

In our case, the i th row of $n \times 2$ design matrix \mathbf{F} , $i = 1, \dots, n$, is defined as

$$\mathbf{f}'_i = \left(\frac{\partial\phi(x_i, \beta_1^0, \beta_2^0)}{\partial\beta_1}, \frac{\partial\phi(x_i, \beta_1^0, \beta_2^0)}{\partial\beta_2} \right), \quad (4)$$

with

$$\begin{aligned} \frac{\partial\phi(x_i, \beta_1^0, \beta_2^0)}{\partial\beta_1} &= \coth(\beta_2^0 \cdot x_i) - \frac{1}{\beta_2^0 \cdot x_i}, \\ \frac{\partial\phi(x_i, \beta_1^0, \beta_2^0)}{\partial\beta_2} &= \frac{-\beta_1^0 \cdot x_i}{[\sinh(\beta_2^0 \cdot x_i)]^2} + \frac{\beta_1^0}{(\beta_2^0)^2 \cdot x_i}. \end{aligned}$$

The matrix \mathbf{H}_i , $i = 1, \dots, n$, is in the form of

$$\begin{pmatrix} 0, & -\frac{x_i}{[\sinh(\beta_2^0 x_i)]^2} + \frac{1}{\beta_2^0 x_i} \\ -\frac{x_i}{[\sinh(\beta_2^0 x_i)]^2} + \frac{1}{\beta_2^0 x_i}, & \frac{2\beta_1^0 x_i^2 \cosh(\beta_2^0 x_i)}{[\sinh(\beta_2^0 x_i)]^3} - \frac{2\beta_1^0}{[\beta_2^0]^3 x_i} \end{pmatrix}.$$

Nevertheless, the quadratic model (3) is still rather complicated. If we neglected also the second derivatives of the Langevin function, i.e., neglecting the quadratic term $\kappa(\delta\beta)$, we would arrive at a linear model given as

$$\bar{y} - \phi(\beta_1^0, \beta_2^0) = \mathbf{F}\delta\beta + \varepsilon. \quad (5)$$

To assess whether the quadratic model (3) can be really linearized it is necessary to verify the consistency between the experimental data and the linearized model (5). More precisely, it is necessary to test the hypothesis if “linearized model (5) is true” against an alternative if “quadratic model (3) is true”, at the significance level α . One possible solution of this problem, based on the Bates and Watts curvature [1], leads to the so-called linearization region [6]. The Bates and

Watts intrinsic curvature of the model (3) at the point β^0 is defined as [1]

$$C^{(int)}(\beta^0) = \sup \{k_M : \delta\beta \in \mathbb{R}^2\},$$

where

$$\begin{aligned} k_M &= \frac{\sqrt{\sigma^2 \kappa'(\delta\beta) \Lambda \mathbf{M}_F^\Lambda \kappa(\delta\beta)}}{\delta\beta' \mathbf{F}' \Lambda \mathbf{F} \delta\beta}, \\ \mathbf{M}_F^\Lambda &= \mathbf{I} - \mathbf{P}_F^\Lambda, \\ \mathbf{P}_F^\Lambda &= \mathbf{F}(\mathbf{F}' \Lambda \mathbf{F})^{-1} \mathbf{F}' \Lambda. \end{aligned}$$

Moreover, let $tol_{\mathcal{L}}$ be a chosen tolerable increase in the significance level α induced by model linearization. Then, the linearization region for consistency between experimental data and linearized model is given as a set defined as

$$\mathcal{L}_{int}(\beta^0) = \left\{ \beta^0 + \delta\beta : \delta\beta' \mathbf{F}' \Lambda \mathbf{F} \delta\beta \leq \frac{2\sigma^2 \sqrt{\delta_{\max}}}{C^{(int)}(\beta^0)} \right\}, \quad (6)$$

where δ_{\max} is the solution of the probabilistic equation given as

$$P\{\chi_{n-2}^2(\delta_{\max}) \geq \chi_{n-2}^2(1-\alpha)\} = \alpha + tol_{\mathcal{L}}.$$

Here the symbol $\chi_{n-2}^2(\delta_{\max})$ denotes a random variable with a non-central chi-squared distribution with $n-2$ degrees of freedom and with the non-centrality parameter δ_{\max} ; $\chi_{n-2}^2(1-\alpha)$ represents the $(1-\alpha)$ -quantile of the central chi-squared distribution with $n-2$ degrees of freedom.

Hence, under assumption of normality, for sufficiently small $tol_{\mathcal{L}}$, the quadratic model (3) can be approximated by the linear model (5) within the linearization region \mathcal{L}_{int} . We explain the practical use of this region in the next section.

To determine the linearization region, the supremum is to be found in order to evaluate the intrinsic curvature. The following simple iterative procedure introduced in [6] can be used. This procedure is based on the original idea proposed by Bates and Watts [1]; however, in this form, the algorithm is modified in order to use the matrices of the first and second derivatives during the calculation directly.

Algorithm 1 (Intrinsic curvature $C^{(int)}(\beta^0)$). *In the first step, we choose an arbitrary vector $\delta\mathbf{u}_1 \in \mathbb{R}^2$ such that $\delta\mathbf{u}_1' \delta\mathbf{u}_1 = 1$. After that, we determine the vector $\delta\mathbf{s}$ defined as*

$$\delta\mathbf{s} = (\mathbf{F}' \Lambda \mathbf{F})^{-1} (\mathbf{H}_1 \delta\mathbf{u}_1, \dots, \mathbf{H}_n \delta\mathbf{u}_1) \Lambda \mathbf{M}_F^\Lambda \kappa(\delta\mathbf{u}_1).$$

Then, we identify the vector $\delta\mathbf{u}_2 = \delta\mathbf{s} / \sqrt{\delta\mathbf{s}' \delta\mathbf{s}}$. In the last step, we verify the inequality given as $\delta\mathbf{u}_2' \delta\mathbf{u}_1 \geq 1 - tol$, where tol is the sufficiently small positive number. If the inequality is satisfied, we terminate the iterative process and the intrinsic curvature is equal to

$$C^{(int)}(\beta^0) = \frac{\sqrt{\sigma^2 \kappa'(\delta\mathbf{u}_2) \Lambda \mathbf{M}_F^\Lambda \kappa(\delta\mathbf{u}_2)}}{\delta\mathbf{u}_2' \mathbf{F}' \Lambda \mathbf{F} \delta\mathbf{u}_2}.$$

If the inequality is not satisfied, we return to the first step of the algorithm where we update the initial vector $\delta\mathbf{u}_1$ by $\delta\mathbf{u}_2$.

There are other types of linearization regions based on the Bates and Watts parametric curvature [1] derived for particular statistical inference [6], e.g., for the bias of the estimator, for a confidence level of confidence domain, etc., however, in practice it is usually sufficient to use above mentioned one. For other approach to test the consistency between data and linearized model, see [11].

2.3. Estimation in linear model

Let us consider the linear model (5), i.e., the model in the form of $\bar{\mathbf{y}} - \phi(\beta_1^0, \beta_2^0) = \mathbf{F}\delta\beta + \varepsilon$, $\delta\beta = \beta - \beta^0$. Recall that $\bar{\mathbf{y}}$ is the n -dimensional normally distributed observation vector with the covariance matrix $\sigma^2\Lambda^{-1}$ such that \bar{y}_i represents an average of three independent measurements at the point x_i , \mathbf{F} is the known design matrix and $\delta\beta$ is the vector of unknown regression parameters.

The best linear unbiased estimator (BLUE) of the regression parameter $\delta\beta$ is given as [9]

$$\widehat{\delta\beta} = (\mathbf{F}'\Lambda\mathbf{F})^{-1}\mathbf{F}'\Lambda[\bar{\mathbf{y}} - \phi(\beta_1^0, \beta_2^0)]. \quad (7)$$

Hence, the BLUE of the parameter β is calculated from

$$\widehat{\beta} = \widehat{\delta\beta} + \beta^0 \quad (8)$$

and its covariance matrix is then given by [9]

$$\text{Var}(\widehat{\beta}) = \sigma^2(\mathbf{F}'\Lambda\mathbf{F})^{-1}. \quad (9)$$

To describe the accuracy and reliability of the estimated values, a confidence domain can be used. The confidence domain for the parameter β is a set in parametric space of β , which covers the true value of β with a given probability of $1 - \alpha$. Explicit formula for $(1 - \alpha)100\%$ -confidence domain for β can be written as [9]

$$\mathcal{E}_{1-\alpha}(\beta) = \left\{ \mathbf{u} \in \mathbb{R}^2 : (\mathbf{u} - \widehat{\beta})'\mathbf{F}'\Lambda\mathbf{F}(\mathbf{u} - \widehat{\beta}) \leq \sigma^2\chi_2^2(1 - \alpha) \right\}. \quad (10)$$

Geometrically, the confidence domain is an ellipse with the center at the estimated point $\widehat{\beta} = (\widehat{\beta}_1, \widehat{\beta}_2)'$. The smaller the area enclosed by the confidence ellipse $\mathcal{E}_{1-\alpha}(\beta)$ is, the more accurate the estimates of β are.

Moreover, the confidence domain for the parameter β is a proper tool for decision whether the model can be linearized or not. The linearization region $\mathcal{L}_{int}(\beta^0)$ is also characterized as an ellipse, however, its center is at the approximate point β^0 . Semi-axes directions are determined by the eigenvector matrix $\mathbf{F}'\Lambda\mathbf{F}$ and are identical for both types of areas $\mathcal{L}_{int}(\beta^0)$ and $\mathcal{E}_{1-\alpha}(\beta)$. Thus, by shifting the center of the linearization region $\mathcal{L}_{int}(\beta^0)$ to the estimated point $\widehat{\beta}$, we obtain simple linearization criterion: The quadratic model can be linearized if the confidence domain $\mathcal{E}_{1-\alpha}(\beta)$ is a subset of the linearization region $\mathcal{L}_{int}(\widehat{\beta})$, i.e., $\mathcal{E}_{1-\alpha}(\beta) \subset \mathcal{L}_{int}$, or, equivalently, if

$$\chi_2^2(1 - \alpha) \leq \frac{2\sqrt{\delta_{\max}}}{C^{(int)}(\beta^0)}.$$

2.4. D-optimal design of the experiment

The main objective of the whole analysis is to obtain the most accurate estimator of the unknown parameter β . To fulfill this objective as much as possible, we construct D-optimal design of experiment (DOE) which secures a minimum area of the confidence ellipse for the parameter β [7].

If $\mathbf{x} = \{x_1, \dots, x_n\}$ is the set of all experimental points, then the function $\delta : \mathbf{x} \rightarrow \langle 0, 1 \rangle$, with the properties such that $\delta(i) = \delta(x_i) \geq 0$, $i = 1, \dots, n$ and $\sum_{i=1}^n \delta(i) = 1$, describes the design of the experiment; the number $\delta(i)$ represents the relative number of measurements at the point x_i . The support of the design is given by the set of experimental points to which a non-zero value was assigned by the design δ , i.e., $\text{Sp}(\delta) = \{x_i : \delta(i) > 0, x_i \in \mathbf{x}\}$. The information matrix of the design δ is defined as

$$\mathbf{M}(\delta) = \sum_{i \in \text{Sp}(\delta)} \delta(i)\lambda_i \mathbf{f}_i \mathbf{f}_i',$$

where \mathbf{f}_i' is the i th row of the design matrix \mathbf{F} (4) and λ_i is the weight of measurement at the point x_i . In our case, $\lambda_i = 1$ and the elements of the information matrix can be calculated using the formulas given as

$$\begin{aligned} M_{11} &= \sum_{i=1}^n \delta_i \cdot \lambda_i \cdot \left(\coth(\beta_2 \cdot x_i) - \frac{1}{\beta_2 \cdot x_i} \right)^2, \\ M_{12} &= M_{21} = \sum_{i=1}^n \delta_i \cdot \lambda_i \cdot \left(\coth(\beta_2 \cdot x_i) - \frac{1}{\beta_2 \cdot x_i} \right) \\ &\quad \times \left(\frac{-\beta_1 \cdot x_i}{[\sinh(\beta_2 \cdot x_i)]^2} + \frac{\beta_1}{\beta_2^2 \cdot x_i} \right), \\ M_{22} &= \sum_{i=1}^n \delta_i \cdot \lambda_i \cdot \left(\frac{-\beta_1 \cdot x_i}{[\sinh(\beta_2 \cdot x_i)]^2} + \frac{\beta_1}{\beta_2^2 \cdot x_i} \right)^2. \end{aligned}$$

If N denotes the total number of all measurements carried out in the experiment, the number of measurements that are performed at the point $x_i \in \text{Sp}(\delta)$ is equal to $r(i) = \delta(i)N$.

Let us consider an arbitrary fixed design δ with the support $\text{Sp}(\delta) = \{x_{i_1}, \dots, x_{i_n}\}$. We denote $\bar{\mathbf{y}}_\delta = (\bar{y}_{i_1}, \dots, \bar{y}_{i_n})'$ as the vector of sample mean magnetization observed at the points x_{i_n} ; particularly \bar{y}_{i_1} is the average of $r(i_1)$ independent measurements at the point x_{i_1} , etc. By using formulas (7)-(9), the BLUE of the parameter β , derived from the experiment carried out according to the design δ , is given as $\widehat{\beta}_\delta = \beta^0 + \widehat{\delta\beta}_\delta$ with the covariance matrix $\text{Var}(\widehat{\beta}_\delta) = \sigma^2(\mathbf{F}'_\delta \Lambda_\delta \mathbf{F}_\delta)^{-1}$, where

$$\widehat{\delta\beta}_\delta = (\mathbf{F}'_\delta \Lambda_\delta \mathbf{F}_\delta)^{-1} \mathbf{F}'_\delta \Lambda_\delta [\bar{\mathbf{y}}_\delta - \phi_\delta(\beta_1^0, \beta_2^0)]. \quad (11)$$

Here \mathbf{F}_δ and $\phi_\delta(\beta_1^0, \beta_2^0)$ are constructed from \mathbf{F} and $\phi(\beta_1^0, \beta_2^0)$, respectively, by omitting rows with indexes to which zero values were assigned by the design δ . The matrix Λ_δ is constructed similarly by omitting rows and columns corresponding to $\delta(i) = 0$, i.e., $\Lambda_\delta = \text{diag}[\lambda_{i_1} r(i_1), \dots, \lambda_{i_n} r(i_n)]$.

The design is said to be D-optimal if and only if it minimizes the determinant of the inverse information matrix [3, 17]. It can be determined by the following iterative procedure [3, 17]:

Algorithm 2 (D-optimal Design). *In the first step, we choose an initial design $\delta_0(i) = 1/k$ with the support $Sp(\delta_0) = \{x_{i_1}, \dots, x_{i_k}\}$. The number of elements in the support $Sp(\delta_0)$ should be greater than or equal to number of estimated regression parameters of β .*

In the following steps, we determine a sequence of designs $\delta_1, \delta_2, \dots$ such that the design δ_{s+1} in the $(s+1)$ -step is a convex combination of the design δ_s from the s -step and the one-point design with the support $\{x_{i_{s+1}^}\}$, where the index i_{s+1}^* is a solution of maximization problem given as*

$$\max \{ \lambda_i \mathbf{f}_i' \mathbf{M}^{-1}(\delta_s) \mathbf{f}_i : i = 1, \dots, n \}.$$

In particular, the support of the design δ_{s+1} is defined as $Sp(\delta_{s+1}) = Sp(\delta_s) \cup \{x_{i_{s+1}^}\}$ and*

$$\delta_{s+1}(i_{s+1}^*) = \begin{cases} \frac{1}{k+s+1} & \text{if } x_{i_{s+1}^*} \notin Sp(\delta_s) \\ \frac{\delta_s(i_{s+1}^*)(k+s)+1}{k+s+1} & \text{if } x_{i_{s+1}^*} \in Sp(\delta_s) \end{cases}$$

$$\delta_{s+1}(i) = \frac{\delta_s(i)(k+s)}{k+s+1} \quad \text{if } x_i \in Sp(\delta_s) \text{ \& } i \neq i_{s+1}^*.$$

Consequently, the information matrix of the design δ_{s+1} is given as the same convex combination of the information matrices of the design δ_s from the s -step and one-point design with the support $\{x_{i_{s+1}^}\}$, i.e.,*

$$\mathbf{M}(\delta_{s+1}) = \frac{k+s}{k+s+1} \mathbf{M}(\delta_s) + \frac{1}{k+s+1} \lambda_{i_{s+1}^*} \mathbf{f}_{i_{s+1}^*} \mathbf{f}_{i_{s+1}^*}'.$$

If the inequality given as

$$\max \{ \lambda_i \mathbf{f}_i' \mathbf{M}^{-1}(\delta_{s+1}) \mathbf{f}_i : i = 1, \dots, n \} < k + tol_D,$$

where k is a number of regression parameters β and tol_D is a chosen tolerance, is satisfied, the algorithm is terminated and the design δ_{s+1} is considered as D-optimal. The points from the initial design which have a relative frequency of measurement tending to zero are omitted from the optimal design.

3. NUMERICAL STUDY

Firstly, we explore the linearization regions in order to decide whether the linearization is possible. Table 1 lists results obtained by linearization of the model, describing the measurement of magnetization in all 150 experimental points. For calculation, we used relations (6) with tolerance $tol_{\mathcal{L}} = 0.01$ and (10).

Before DOE	Semi-axis	Results of right side
\mathcal{L}_{int}	0.0096 $14.0150 \cdot 10^{-6}$	$\delta_{max} = 2.6129$ $C^{int} = 0.0098$
$\mathcal{E}_{0.95}(\beta)$	0.0013 $1.8888 \cdot 10^{-6}$	$\chi_2^2(0.95) = 5.9900$

Tab. 1: Linearization region and 95% confidence domain for β . Model before DOE.

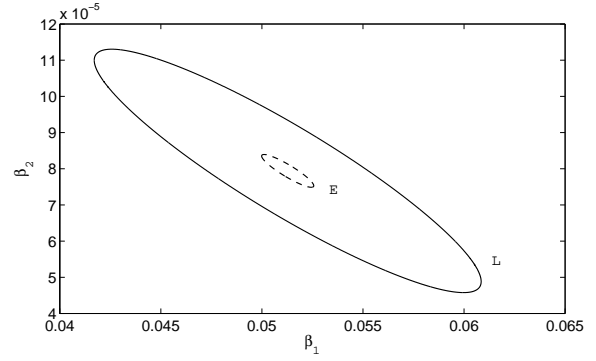


Fig. 2: Linearization region (dashed line) and 95% confidence domain (solid line). Model before DOE.

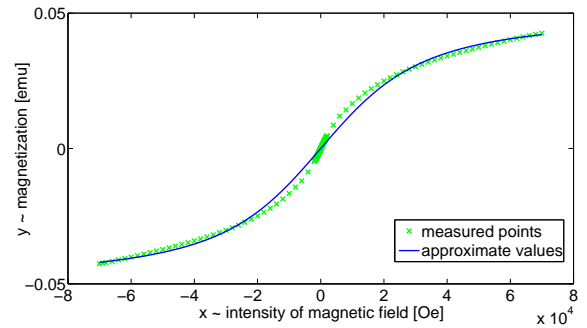


Fig. 3: Approximation of the measured values by the Langevin function before using DOE.

Since $\chi_2^2(0.95) = 5.99 < 2\sqrt{\delta_{max}/C^{int}} = 329.7986$, the confidence domain lies within the linearization region (see Fig. 2) and thus the linearization of model is possible.

The estimates of parameter β and their standard errors in the linearized model are $\hat{\beta}_1 = 0.0513 \pm 0.0005$ and $\hat{\beta}_2 = 7.94 \cdot 10^{-5} \pm 0.19 \cdot 10^{-5}$. Substituting the estimates into Langevin function (1), we get an approximation \hat{y} illustrated in Fig. 3. We can quantify the goodness-of-fit of the model by, for example, the coefficient of determination R^2 . It is defined as [9] $R^2 = 1 - SSE/SST$, where $SSE = (\bar{y} - \hat{y})' \Lambda (\bar{y} - \hat{y})$ is the residual sum of squares and $SST = (\bar{y} - m1_n)' \Lambda (\bar{y} - m1_n)$ is the total sum of squares. Here $m = (1/n) \sum_{i=1}^n \bar{y}_i$ and 1_n is the vector formed by n ones. In our case, $R^2 = 0.996$.

The above-presented experiment was realized at all 150 points of the experimental set. These points were spaced symmetrically but not equidistantly. Most measurements were distributed from -20000 to $+20000$ Oe. Then, we attempted to search for the D-optimal design of nanomaterial's magnetization measurement. We determined the starting design of measurement δ_0 with two points $\{x_7, x_{150}\} = \{-60000, 70000\} \in \mathbf{x}$ which formed the support of the starting design δ_0 .

The D-optimal experiment design chooses two points that can be considered as optimal points for the measurement as

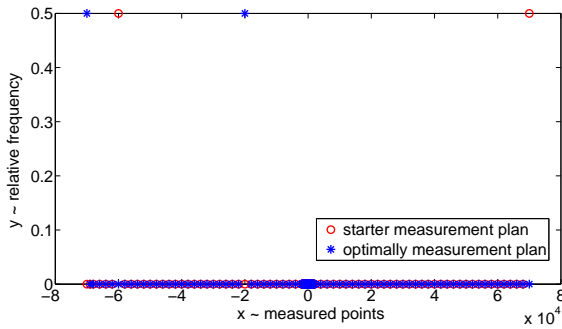


Fig. 4: D-optimal design of the experiment for the measurement of the Langevin function.

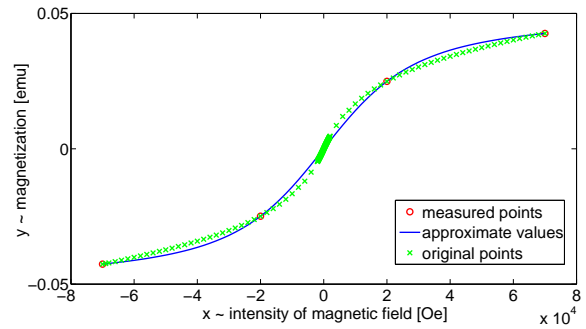


Fig. 5: Approximation of the measured values by the Langevin function after using DOE.

shown in Fig. 4. We determined the frequency of the measurement in these points as it is shown in Tab. 2.

DOE	Points	Frequency
Initial design	$\delta_0(x_7) = 0.5$	$r_{x_7} = 225$
δ_0	$\delta_0(x_{150}) = 0.5$	$r_{x_{150}} = 225$
Optimal design	$\delta^*(x_1) = 0.498$	$r_{x_1} = 225$
δ^*	$\delta^*(x_{27}) = 0.499$	$r_{x_{27}} = 225$

Tab. 2: D-optimal design of the experiment.

Since the function (1) is symmetric, we divided the relative measurement frequencies both into two optimal points $\{x_1, x_{27}\} = \{-70000, -20000\}$ and into points $\{x_{125}, x_{150}\} = \{20000, 70000\}$. Then, we split the original 450 measurements into four optimal points $r(x_1) = 112$, $r(x_{27}) = 113$, $r(x_{125}) = 113$, and $r(x_{150}) = 112$ in a proportion of the relative measurement frequency.

We carried out new measurement of the same sample made up of $\gamma\text{-Fe}_2\text{O}_3$ nanoparticles, however, this time, we performed the measurements only at the optimal points of the external magnetic field. As clearly seen, the estimates obtained from the model before DOE and after DOE are almost the same. Namely, we compared the confidence domain of both models and subsequently evaluated the effect of the D-optimal criterion. Results of these measurements are summarized in Tab. 3.

After DOE	Semi-axis	Results of right side
\mathcal{L}_{int}	19.8663 0.0456	$\delta_{max} = 2.6129$ $C^{int} = 4.18 \cdot 10^{-10}$
$\mathcal{E}_{0.95}(\beta)$	$5.5287 \cdot 10^{-4}$ $1.2701 \cdot 10^{-6}$	$\chi_2^2(0.95) = 5.99$

Tab. 3: Linearization region and 95% confidence domain for β . Model after DOE.

The change in the design significantly affected the Bates and Watts intrinsic curvature of the model. After DOE, the confidence domain also lies within the linearization region as expected, i.e., $\chi_2^2(0.95) = 5.99 < 2\sqrt{\delta_{max}}/C^{int} = 7.73 \cdot 10^9$. The estimates of parameter β and their standard errors in the linearized model are $\hat{\beta}_1 = 0.0510 \pm 0.0002$ and $\hat{\beta}_2 = 8.70 \cdot 10^{-5} \pm 0.09 \cdot 10^{-5}$. $R^2 = 1$ with respect to measurements

according to DOE and $R^2 = 0.996$ with respect to the original measurements. Approximation of the Langevin function using DOE \hat{y}_D is depicted in Fig. 5.

It is clear that the variance of estimates obtained using DOE is smaller than the variance of estimates obtained from the initial model. The D-optimal criterion leads to the minimization of the confidence domain of the unknown vector parameter estimator and therefore, we arrive at more accurate estimates. Approximated Langevin functions are almost the same for both experiments (the sum of squared differences of fitted values in original points x_1, \dots, x_n is less than 0.00005), however, the experiment carried out according to DOE is simpler.

Analytical course of the Langevin function does not copy the course of magnetization perfectly (see Fig. 3. and Fig. 5.). This is the reason why we can expect that the parameter estimates obtained from different designs will be slightly different. Relation of the Langevin function is strictly given. Slight differences in the estimations caused by the choice of different designs could be neglected from the practical viewpoint. However, improvement of the analytical form is the subject of further research.

4. CONCLUSIONS

At present, the nanosized materials are of eminent interest both from fundamental and applied reasons. However, their research, synthesis, analysis, and characterization are very money-consuming and therefore, it is highly needed to achieve the most accurate results and effective approaches. In order to get the estimators of the unknown parameters, we used the theory of nonlinear regression models which provide not only the estimators themselves but also their accuracy. This is the main goal for the physical characterization of nanoparticle samples as precise knowledge of these parameters predestinates nanomaterials for their future possible application.

To find the most effective approach, we used the theory of optimal design of experiments. We used the D-optimal criterion to minimize the volume of confidence domain of the unknown parameters. It turned out that it is absolutely suffi-

cient to carry out the magnetization measurement only at four optimal points as we get the same values of the unknown parameters estimators but with a higher accuracy. This represents the most important outcome of our presented approach. The additional very important profit of the presented work lies in a decrease in the cost of the measurement as demonstrated in Tab. 4.

	Before DOE	After DOE
Number of stabilization processes	150	4
Measuring time	5h 25 min	0h 48 min
Helium consumption	3.1 l	0.7 l
Operating costs	34 EURO	5.6 EURO
Price of helium	33 EURO	7.7 EURO
Total costs	67 EURO	13.3 EURO

Tab. 4: Cost savings obtained by application of DOE.

5. ACKNOWLEDGEMENTS

This work was supported by the Grant No. PrF-2012-017 and No. PrF-2012-008 of the Internal Grant Agency of the Palacky University in Olomouc and by the Operational Program Research and Development for Innovations – European Regional Development Fund (CZ.1.05/2.1.00/03.0058).

REFERENCES

- [1] Bates, D.M., Watts, D.G. (2008). *Nonlinear regression analysis and its applications*, Wiley.
- [2] Dormann, J.L., Fiorani, D., Tronc, E. (1997). Magnetic relaxation in fine-particle systems, *In: Advances in Chemical Physics, I. Prigogine*, John Wiley and Sons, New York, Vol. 98, 283–494.
- [3] Fedorov, V.V. (1972). *Theory of optimal experiments*, Academic Press.
- [4] Kluchova, K., Zboril, R., Tucek, J., Pecova, M., Zajoncova, L., Safarik, I., Mashlan, M., Markova, I., Jancik, D., Sebela, M., Bartonkova, H., Bellesi, V., Novak, P., Petridis, D. (2009). Superparamagnetic maghemite nanoparticles from solid-state synthesis - Their functionalization towards peroral MRI contrast agent and magnetic carrier for trypsin immobilization. *Biomaterials* 30, 2855–2863.
- [5] Kodama, R.H. (1999). Magnetic nanoparticles. *J. Magn. Mater.* 200, 359–372.
- [6] Kubáček, L., Tesaříková, E. (2009). *Weakly nonlinear regression models*, UP Olomouc.
- [7] Kubáčková, L., Kubáček, L., Kukuča, J. (1987). *Probability and statistics in geodesy and geophysics*, Elsevier, Amsterdam-Oxford-New York-Tokyo.
- [8] Machala, L., Tucek, J., Zboril, R. (2011). Polymorphous transformations of nanometric iron(III) oxide: A review. *Chem. Mater.* 23, 3255–3272.
- [9] Montgomery, D.C., Peck, E.A., Vining, G.G. (2006). *Introduction to linear regression analysis*, 4th ed., John Wiley and Sons, Inc., Hoboken, New Jersey.
- [10] O’Handley, R.C. (2000). *Modern magnetic materials: Principles and applications*, John Wiley and Sons, New York.
- [11] Pázman, A. (1993). *Nonlinear statistical models*, Kluwer Academic Publisher, Dodrecht-Boston-London and Ister Science Press, Bratislava.
- [12] Poole, Ch.P., Owens, F.J. (2003). *Introduction to nanotechnology*, John Wiley & Sons, New Jersey.
- [13] Strbak, O. Kopcansky, P., Frollo, I. (2011). Biogenic magnetite in humans and new magnetic resonance hazard questions. *Measurement Science Review*, Volume 11, No. 3., 85–91.
- [14] Tucek, J., Zboril, R., Petridis, D. (2006). Maghemite nanoparticles by view of Mössbauer spectroscopy. *J. Nanosci. Nanotechnol.* 6, 926–947.
- [15] Tucek, J., Zboril, R., Namai, A., Ohkoshi, S. (2010). ϵ -Fe₂O₃: An advanced nanomaterial exhibiting giant coercive field, millimeter-wave ferromagnetic resonance, and magneto-electric coupling. *Chem. Mater.* 22, 6483–6505.
- [16] Tučková, M., Tuček, P., Tuček, J., Kubáček, L. (2010). Search for optimal way to precisely evaluate magnetic response of ironoxide based nanomaterials-a new statistically-based approach. *Nanocon 2010, 2nd International Conference*, 478–484.
- [17] Wynn, H.P. (1972). Results in the theory and construction of D-optimum experimental designs. *Journal of the Royal Statistical Society*, Vol. 34, No. 2, 133–147.
- [18] Zboril, R., Mashlan, M., Petridis, D. (2002). Iron(III) oxides from thermal processes-synthesis, structural and magnetic properties, Mossbauer spectroscopy characterization and applications. *Chem. Mater.* 14, 969–982.

Received March 29, 2012.

Accepted August 3, 2012.